J Appl Electrochem (2009) 39:2191–2197
DOI 10.1007/s10800-008-9767-0

ORIGINAL PAPER

Electrodeposition of PbS multilayers on Ag(111) by ECALE

V. C. Fernandes · E. Salvietti · F. Loglio · E. Lastraioli · M. Innocenti · L. H. Mascaro · M. L. Foresti

Received: 3 October 2008 / Accepted: 18 December 2008 / Published online: 14 January 2009

Abstract Lead sulfide (PbS) thin films were grown on a single crystal Ag(111) substrate by Electrochemical Atomic Layer Epitaxy (ECALE) method, i.e., by alternated underpotential deposition (UPD) of lead and sulfur. The electrochemical analysis includes the investigation of the underpotential deposition processes of both Pb and S, and the characterization of deposits obtained with different deposition cycles to confirm the attainment of the right stoichiometric ratio between Pb and S. The morphological analysis has been performed by Atomic Force Microscopy (AFM) for deposits formed with 50 and 75 deposition cycles and at different times of exposition to the atmosphere.

Keywords PbS · ECALE · Electrodeposition · AFM · Ag(111)

1 Introduction

Binary semiconductors are considered important technological materials because of their potential applications in optoelectronic devices, solar cells, IR detectors, and lasers [1, 2]. Binary compounds of group IIB and group VIA elements, commonly referred to as II–VI compounds, have important technological applications. Thin films of these compounds are usually prepared by vacuum evaporation, chemical vapor deposition, sputtering and spray pyrolysis methods [3, 4]. The crucial point in material electrodeposition is to control the dimensions of the electrodeposited structures. The great interest in nanometer-scale materials stems from the fact that their optical, electrical, magnetic, or mechanical properties are often very different from the same materials in the bulk phase, and, more importantly, they can be tuned by changing the physical dimensions of the material. Of course, compound electrodeposition also requires composition control, that is to say the right stoichiometric ratio. Combining dimensional and composition control allows the attainment of compound semiconductor thin films, which is our field of interest. The semiconductive layers of electronics and optoelectronics devices must be, if possible, crystalline and, still better, epitaxial. In fact, small amounts of stress can shift the luminescent properties, and a small number of defects can provide recombination centers that lower the device's efficiency. For this purpose, the Electrochemical Atomic Layer Epitaxy (ECALE) technique developed by Stickney [5] is a valid approach for the attainment of II–VI compound semiconductors on metallic substrates.

The method is based on the alternate underpotential deposition of atomic layers of the elements that form the compound, in a cycle that can be repeated as many times as desired. The major advantage of this method is that the individual steps of each cycle can be examined and optimized independently. This means that the conditions for deposition can be adjusted according to potentials, pH, reactants, and so on. These conditions are strictly dependent on the compound that must be obtained, and on the substrate used. Of course, the use of single crystal substrates increases the probability of the epitaxial growth. Electrochemical Atomic Layer Epitaxy (ECALE) has been

V. C. Fernandes · L. H. Mascaro
Departamento de Química, Universidade Federal de São Carlos, Caixa Postal 676, Sao Carlos, SP 13565-905, Brazil

E. Salvietti · F. Loglio · E. Lastraioli · M. Innocenti · M. L. Foresti (✉)
Department of Chemistry, University of Florence, Via della Lastruccia 3, 50019 Sesto Fiorentino (FI), Italy
e-mail: foresti@unifi.it

used to produce a wide variety of well-ordered semiconductor deposits under ambient pressure and temperature [6]. In our laboratory both binary and ternary sulfides of cadmium and zinc have been studied [7–11].

Lead sulfide (PbS) is a binary semiconductor that has received considerable attention because of its variety of applications. In fact, due to its direct band gap of 0.37 eV and absorption coefficient which continuously increase from the infrared through the visible region, PbS has been used in infrared detectors since the mid 1940s [12]. Like most heavy metal chalcogenides, it seems to be a promising sensor material, particularly for nitrogen oxides [13]. The techniques commonly used to produce PbS thin films are: electrodeposition [14, 15], successive ionic layer absorption and reaction (SILAR) [16, 17] and chemical bath deposition (CBD) [18]. A few attempts have been made to investigate the PbS by ECALE method [19–21]. This paper concerns the preparation of PbS grown by ECALE method and its electrochemical and morphological characterization.

2 Experimental

For electrochemical deposition of thin semiconductor films, analytical reagent grade was used, without further purification. Merck $Pb(NO_3)_2$ and Aldrich Na_2S were used as sources of Pb and S, respectively. $HClO_4$ (Merck) and NH_4OH (Merck) were used to prepare the pH 9.6 ammonia buffer, whereas $CH_3COONa \cdot 3H_2O$ (Merck) and CH_3COOH (Merck) were used to prepare the pH 5.0 acetic buffer used as supporting electrolyte. The water used was obtained from mineral water by distilling it once and then, re-distilling it again in alkaline permanganate medium while constantly discarding the heads. The solutions were freshly prepared just before the beginning of each series of measurements.

An automated deposition apparatus, consisting of Pyrex solution reservoirs, solenoid valves, a distribution valve and a flow-cell, which was connected to a computer, was used. Both the distribution valve and the cell were designed and realized in the workshop of the Department of Chemistry of Florence University. The electrolytic cell was a Teflon cylinder with about 7 mm inner diameter and 42 mm outer diameter, whose inner volume, 0.5 ml, was delimited by the working electrode (WE) on one side and the counter electrode (CE) on the other side. The inlet and the outlet for the solutions were placed on the side walls of the cylinder. The CE was Platinum foil, and the reference electrode (RE) was Ag/AgCl/sat. KCl placed on the outlet tube. The distance between reference and working electrodes introduces resistive contributions that cannot be compensated. However, this cell design with the counter electrode facing the working electrode ensures a high homogeneity of the deposits. The silver single crystals were prepared according to the Bridgeman technique and polished by a CrO_3 based procedure [22–24].

AFM images were taken with a commercial instrument (PicoSPM, Molecular Imaging) in contact mode with commercial Si_3N_4 cantilever (Nanosensors, Wezlar–Blankenfield).

3 Results and discussion

The growth of PbS multilayer by ECALE exploits the UPD processes of Pb on S and of S on Pb. The negative Gibbs energy change involved in the formation of the compound is the principal reason for the occurrence of the UPD of Pb on the previously deposited S or vice versa. However, the first atomic layer is formed on the substrate; hence, it is necessary that at least one of the elements forming the compound is deposited on single crystal Ag(111) by a surface limited process. In principle, the semiconductor might be obtained by depositing either the metal or the chalcogen as the first layer. Therefore, for the study of the deposition of the PbS multilayers, the elements were initially examined individually to determine the appropriate conditions for the deposition of the semiconductor.

3.1 Formation of Pb and S atomic layers

The Pb_{UPD} layer on Ag (111) was performed from 5.0 mM $Pb(NO_3)_2$ solutions in acetic buffer of pH 5, by scanning the potential from −0.2 V to −0.45 V (Fig. 1).

Two well-defined and narrow peaks were observed at −0.35 V (B1) and −0.29 V (B2) related to the deposition and dissolution of Pb monolayer, respectively. Here,

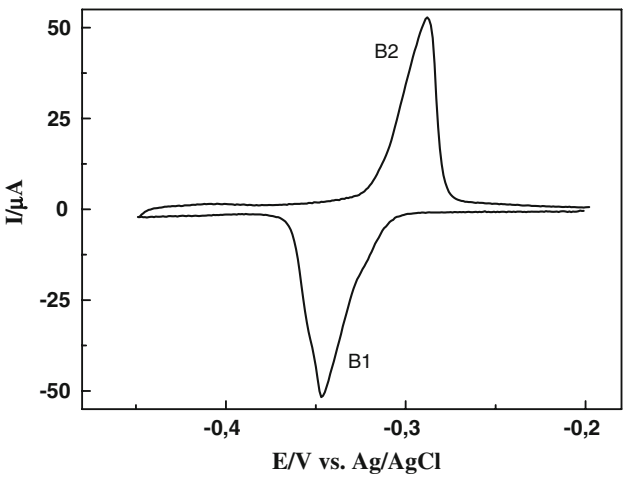

Fig. 1 Cyclic voltammogramm of 5.0 mM $Pb(NO_3)_2$ in pH 5.0 acetate buffer on Ag(111) substrate, v = 10 mV s^{-1}

the difference between the cathodic and anodic peak is somewhat greater than expected, probably due to the uncompensated resistance. However, the shape of cyclic voltammogram of Fig. 1 is consistent to that reported in the literature for the UPD process of lead in acetate medium which is a strong adsorbing electrolyte. In fact, as stressed in Ref. 25 (and references therein), the electrolyte composition and the presence of adsorbing anion have a significant influence on the UPD process.

The constancy of the anodic stripping curves of Pb deposited at −0.45 V and at different accumulation times ensures that the process is surface limited (Fig. 2). Integration of this re-dissolution peak yields a charge value of 332 μC cm^{-2}, which is very close to the value, about 320 μC cm^{-2}, calculated for a hexagonal Pb monolayer with a near-neighbor distance of 3.4 Å upon assuming a two electron charge transfer. This near-neighbor distance is that which corresponds to the potential region immediately preceding bulk deposition: at more positive potentials it has been found to slightly and progressively increase [25].

The underpotential deposition of sulfur on Ag(111) in ammonia buffer has already been extensively investigated and utilized by our group for the attainment of both binary and ternary sulfides [7–11].

Here, it is worthwhile to report that the pH 5 acetic buffer necessary to keep lead in solution could cause a partial re-dissolution of a S monolayer deposited on Ag(111). Curve *a* in Fig. 3 is the stripping curve of S_{UPD} in ammonia buffer after the electrode has been previously kept for 2 min at −0.1 V in acetic buffer. For comparison, the figure also reports the curves obtained without the washing step with acetic buffer (curve *b*) and that performed in acetic buffer (curve *c*). Both curves *a* and *c* show a bump in correspondence of the potential of bulk sulfur dissolution. Taking into account the expected shift of the potential due to the different pH, the bump seems to be connected with a partial re-dissolution of the S monolayer induced by acidic medium.

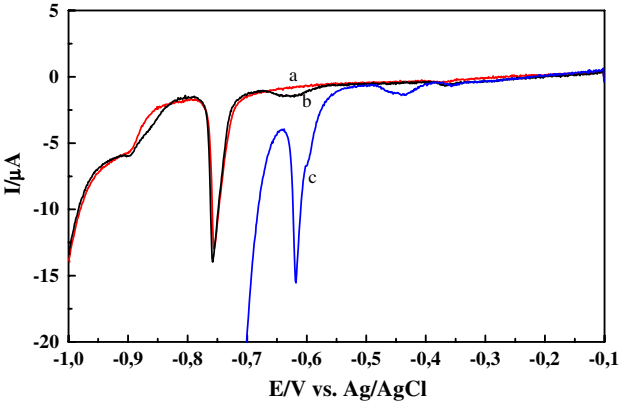

Fig. 3 Stripping curve of S_{UPD} in ammonia buffer after the electrode has been previously kept for 2 min at −0.1 V in acetic buffer (curve *a*). Stripping curve of S_{UPD} without the washing step with acetic buffer (curve *b*) and stripping curve of S_{UPD} performed in acetic buffer (curve *c*)

A more favorable situation is encountered when Pb is chosen as the first element to be deposited on Ag. In fact, in this case all S layers are deposited on Pb, and the much more negative free energy change involved in PbS formation, −23.6 kcal mol^{-1}, than in Ag_2S, −9.72 kcal mol^{-1}, should eliminate the problem of a possible partial re-dissolution of S.

Next, the underpotential deposition of S on a Pb-covered Ag (111) was examined. Figure 4 shows the oxidative underpotential deposition of sulfur on a Pb-covered Ag(111) as obtained by scanning the potential from −1.0 to −0.70 V in 2.5 mM Na_2S solutions in ammonia buffer.

As expected, due to the more negative free energy change, the sulfur UPD process on the Pb-covered Ag(111) occurs at more negative potentials than on Ag(111) [7, 8].

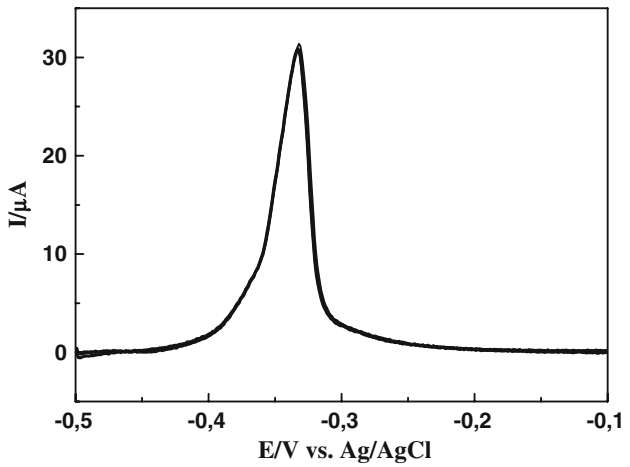

Fig. 2 Coincidence of the stripping curves of Pb_{UPD} deposited at −0.45 V for 45, 60, and 90 s

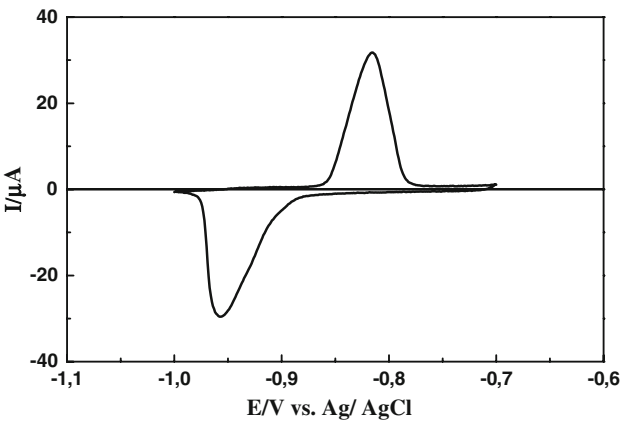

Fig. 4 Cyclic voltammogramm of 2.5 mM Na_2S in pH 9.6 ammonia buffer on a Pb/Ag(111), v = 10 mV s^{-1}

Therefore, the potential chosen for the deposition of S was −0.7 V. Stripping curves of S deposited at −0.7 V for different times showed that the UPD process is completed after 60 s.

The basic ECALE cycle for PbS deposition is then:

- deposition of Pb at −0.45 V for 60 s
- washing at −0.45 V with acetic buffer
- deposition of S at −0.7 V for 60 s
- washing at −0.7 V with ammonia buffer

The cycle is then repeated as many times as necessary to obtain thicker deposits.

3.2 Electrochemical characterization

As usual, the first characterization of the compound obtained is the electrochemical characterization [8] which is carried out, in situ, by scanning the potential to values where the deposits are destroyed. The charge involved in the stripping of the single elements gives the amount of deposition. The first PbS layer was then examined by scanning the potential toward positive values to dissolve Pb and successively toward negative potentials to dissolve S. Between the two scans, the cell was rinsed with the supporting electrolyte to eliminate the dissolved lead ions thus avoiding lead re-deposition.

Curve *b* in Fig. 5 is the stripping curve of Pb from this first PbS monolayer, whereas curve *a* is the stripping curve of Pb directly deposited on Ag(111) as in Fig. 2. As expected, more energy is required to strip Pb from PbS than from the silver substrate. As a consequence, the solid curve is shifted toward more positive potentials.

However, the charge involved in the stripping of Pb from PbS, 296 μC cm^{-2}, amounts to about 92% of that, 332 μC cm^{-2}, measured in the stripping of Pb deposited on

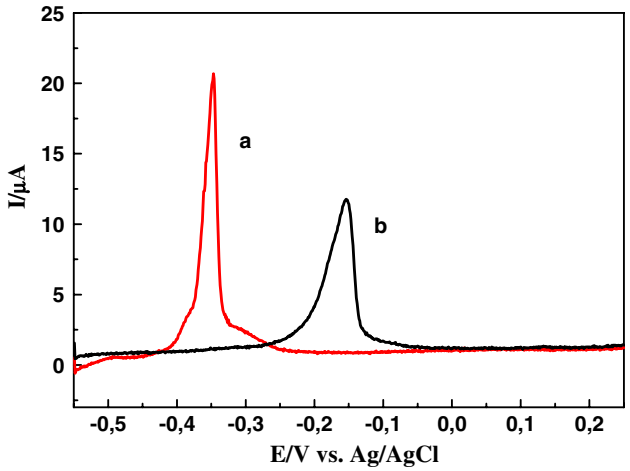

Fig. 5 Stripping curve of Pb from the first PbS monolayer (b); stripping curve of Pb directly deposited on Ag(111) (a), v = 5 mV s^{-1}

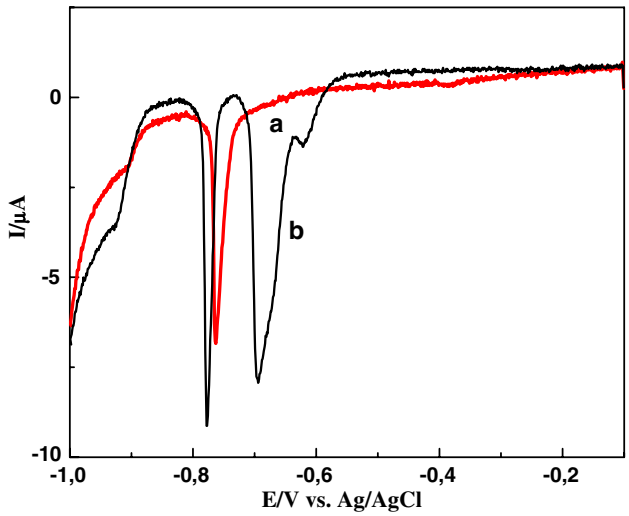

Fig. 6 Stripping curve of the sulfur remaining after lead dissolution (b) and the stripping curve of sulfur directly deposited on Ag(111) (a), v = 5 mV s^{-1}

silver. This could be explained either with a partial destruction of Pb monolayer operated by S deposition or, on the contrary, with the not complete re-dissolution of Pb. The second hypothesis could be supported by the comparison between the stripping curve of the sulfur remained after lead dissolution (curve *a* in Fig. 6) and the stripping curve of sulfur directly deposited on Ag(111) (curve *b* in Fig. 6). The splitting of curve *b* into two peaks is due to the fact that after lead dissolution the amount of remaining sulfur exceeds that corresponding to a UPD layer on Ag(111), and this excess is stripped at the potential of bulk sulfur. Finally, the S stripped at the more negative potential is the UPD peak, but the comparison with the curve *a* indicates that the Ag(111) substrate has been somehow modified either by the formation of a Pb adlayer or even by the formation of a Pb–Ag alloy [26].

The presence of different sites also seems to be suggested by the presence of the small bump preceding the "bulk" S stripping peak. However, only qualitative hypotheses can be formulated on the basic voltammograms that should be supported by more suitable surface analysis tools.

The charge associated to this UPD peak, 66 μC cm^{-2}, plus the charge involved in the "bulk" peak, 260 μC cm^{-2}, gives a charge value, 326 μC cm^{-2}, very close to that, 332 μC cm^{-2}, involved in the stripping of Pb_{UPD} layer deposited on the bare Ag(111).

The charge involved in the stripping of deposits obtained with different numbers of basic ECALE cycles gives the amount of the elements deposited for that number of cycles. The stripping curves of deposits obtained with 2, 5, 10, and 15 cycles are reported in Fig. 7. As usual, the stripping process of the first element (in our case Pb)

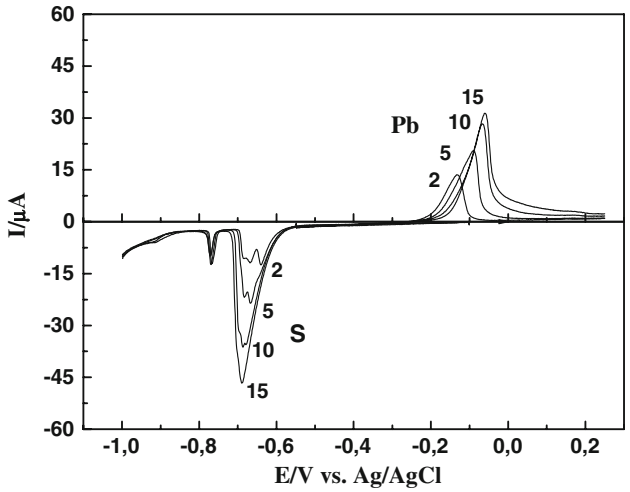

Fig. 7 Linear-sweep voltammograms for the Pb oxidative stripping, and for the S reductive stripping of PbS films deposited with 2, 5, 10, and 15 ECALE cycles, v = 5 mV s^{-1}

becomes progressively more difficult as the number of deposition cycles increases. As has been shown before [8] this is not due to the slow kinetics of the dissolution process, but rather to an increasing stability of the compound that determines a potential shift of the peaks. Once all of the first element has been stripped away, the remaining layers of the second element (in our case S) behave as a bulk deposit. Therefore, they are stripped at the bulk potential except for the first layer, i.e., the layer in contact with the silver substrate. The charge involved in this first layer is constant, regardless of the number of cycles employed. Therefore, this first layer can be considered as the UPD layer.

The behavior described is general and it is fulfilled also by changing the order of the stripping processes. Of course if S is stripped as the first element, the potential shifts in the opposite direction still indicating an increasing stability involved in the compound formation.

Note that the bump observed in Fig. 6 is replaced by a well-defined peak for the deposits obtained with 2 and 5 cycles. However, for deposits obtained with 15 cycles, the two "bulk" peaks merge, thus indicating that the dissolution process is no longer able to distinguish between different sites. Of course this fine structure of the "bulk" S deposit is only observed at low scan rates.

The charges involved in Pb stripping for a given number of cycles coincide with the corresponding charges of sulfur, thus indicating the right 1:1 stoichiometric ratio. Moreover, the plots of the charges for Pb and S stripping as a function of the number of cycles are linear with an average charge per cycle of approximately 83 μC cm^{-2}, suggesting layer-by-layer growth. This behavior is also observed for other semiconductors obtained by ECALE method [8].

3.3 Morphological characterization

The morphological analysis carried out by ex-situ AFM measurements on prepared samples obtained with 50, 75, 100, and 125 ECALE cycle revealed that all samples consisted of homogeneous films of PbS small clusters. However, when exposed to the atmosphere, these clusters tend to enlarge. The morphological evolution of PbS deposits as a function of the exposure time in air was then investigated. The analysis was performed on deposits formed with 50 and 75 deposition cycles and at different times of exposition to the atmosphere.

Figure 8 shows 5 × 5 μm AFM images of a 50 cycle sample as obtained after 1, 16, 40, and 160 h. All images show that the surface is homogeneously covered by a film of PbS clusters of progressively increasing in diameter.

The evolution in time can be well checked through the evaluation of the root mean square roughness parameter (RMS) provided by the AFM software. RMS roughness was calculated via the standard formula:

$$\mathrm{RMS}^2 = (1/\mathrm{N})\Sigma_{ij}\left[\mathrm{h}_{ij} - \hat{h}\right]^2 \quad (1)$$

Here, N is the number of pixels in the image, h_{ij} is the local height at pixel ij, and $\hat{h}$ is the mean height.

The plot of the RMS values calculated on the AFM images of Fig. 8 shows that RMS reaches a limiting value after about 40 h (curve *a* in Fig. 9). Apart from the different limiting value, the same behavior was shown by a sample formed with 75 cycles (curve *b*). This behavior can be related to an initial process of oxidation PbS film [27, 28].

4 Conclusions

PbS thin films were obtained by Electrochemical Atomic Layer Epitaxy (ECALE) method, i.e., by alternated underpotential deposition (UPD) of lead and sulfur. The analysis of the UPD processes of both S and Pb on Ag(111) suggested the deposition of Pb as the first element. The electrochemical characterization was performed on the first PbS layer by the stripping of Pb followed by the stripping of S. The charge measured in the Pb stripping was slightly smaller than expected, thus suggesting an incomplete re-dissolution. A small potential shift observed in the stripping of S suggested that the limited amount of undissolved Pb could somehow modify the silver. However, the electrochemical characterization of deposits formed with an increasing number of deposition cycles up to 15 confirmed the layer-by-layer growth of PbS with the right 1:1 stoichiometric ratio.

The morphological analysis carried out by ex-situ AFM measurements on as prepared samples obtained with 50,

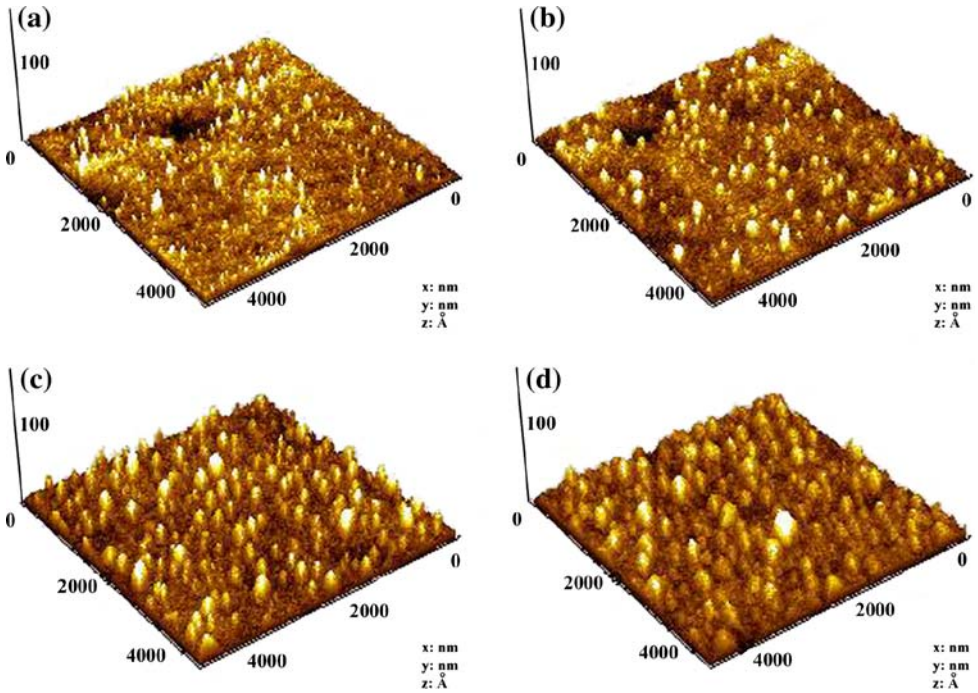

Fig. 8 AFM 5 × 5 μm image of a sample formed with 50 deposition cycles of PbS on Ag(111) as a function of the exposure time in air. **a** 1 h, **b** 16 h, **c** 40 h and **d** 160 h

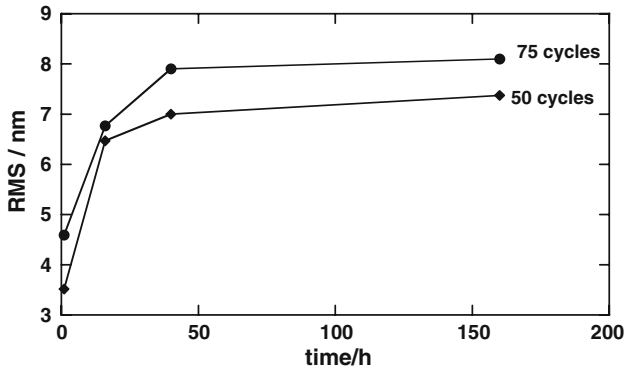

Fig. 9 Plot of RMS roughness of a sample formed with 50 and 75 deposition cycles of PbS on Ag(111) as a function of the exposure time in air

75, 100, and 125 ECALE cycle revealed that all samples consisted of homogeneous films of small PbS clusters. However, when exposed to the atmosphere, these clusters tend to enlarge. In fact, during the first few hours of exposure of the PbS film, the roughness increases rapidly, but after about 40 h it reaches an almost constant value. This behavior can be related to the initial process of oxidation of PbS film. Future work will be devoted to the investigation of optical properties of these films to evaluate their potential applications in optoelectronic devices.

Acknowledgments The authors gratefully acknowledge the Brazilian research funding institutions, CAPES, FAPESP and Fondazione Monte dei Paschi di Siena (Italy).

References

1. Riveros G, Gomez H, Henriguez R, Schrebler R, Maratti RE, Dalchiele EA (2001) Sol Energy Mater Sol Cells 70:255
2. Kumar V, Sharma TP (1998) Opt Mater 10:253
3. Su B, Choy KL (2000) Thin Solid Films 102:361
4. Caicedo LM, Cediel G, Dussan A, Sandino JW, Calderon C, Gordillo G (2000) Phys Status Solidi B 220:249
5. Gregory BW, Stickney JL (1991) J Electronanal Chem 300:543
6. Stickney JL (1999) In: Bard AJ, Rubistein I (eds) Electroanalytical chemistry, vol 21. M. Dekker press, New York, pp 75–209
7. Foresti ML, Pezzatini G, Cavallini M, Aloisi G, Innocenti M, Guidelli R (1998) J Phys Chem B 102:7413
8. Innocenti M, Pezzatini G, Forni F, Foresti ML (2001) J Electrochem Soc 148(5):C357
9. Innocenti M, Cattarin S, Cavallini M, Loglio F, Foresti ML (2002) J Electroanal Chem 53:2219
10. Loglio F, Innocenti M, Pezzatini G, Foresti ML (2004) J Electroanal Chem 562:117
11. Innocenti M, Cattarin S, Loglio F, Cecconi T, Seravalli G, Foresti ML (2004) Electrochim Acta 49:1327
12. Meldrun FC, Flath J, Knoll W (1999) Thin Solid Films 348:188
13. Markov VF, Maskaeva LN (2001) J Anal Chem 56:754
14. Mady AK, Girgis A, Mady AH, Moustaf R (1987) Phys Status Solidi A 100:107
15. Sharon M, Ramaiah KS, Kumar M, Neumann-Spallart M, Levy-Clement C (1997) J Electroanal Chem 436:49
16. Puiso J, Lindroos S, Tamulevicius S, Leskela M, Snitka V (2003) Thin Solid Films 428:223
17. Kanniainen T, Lindroos S, Resch R, Leskela M, Friedbacher G, Grasserbauer M (2000) Mater Res Bull 35:1045
18. Gadave KM, Jodgudri SA, Lokhande CD (1994) Thin Solid Films 245:7
19. Torimoto T, Takabayashi S, Mori H, Kuwabata S (2002) J Electroanal Chem 522:33
20. Őznülüer T, Erdoĝan I, Şişman I, Demir Ü (2005) Chem Mater 17(5):935

21. Fernandes VC, Salvietti E, Loglio F, Innocenti M, Mascaro LH, Foresti ML (2007) ECS Trans 11(7):279
22. Hamelin A (1985) In: White Conway RE, Bockris JO'M (eds) Modern aspects of electrochemistry, vol 16. Plenum Press, New York
23. Kurasawa T (1960) Patent Japan 35:5619
24. Foresti ML, Capolupo F, Innocenti M, Loglio F (2002) Crystal growth and design 2:73–77
25. Toney M, Gordon JG, Samant MG, Borges GL, Melroy OR, Yee D, Sorensen LB (1995) J Phys Chem 99:4733 (and references therein)
26. Sackmann J, Bunk A, Potschke RT, Staikov G, Lorenz W (1998) Electrochim Acta 43:2863
27. Nowak P, Laajalehto K (2000) Appl Surf Sci 157:101
28. Mikhlin YL, Romanchenko AS, Shagaev AA (2006) Appl Surf Sci 252:5645